Influence of neutral transport on ion chemistry uncertainties in Titan ionosphere

N. Carrasco[1,2] , E. Hébrard[3] , M. Banaszkiewicz[4], M. Dobrijevic[5] , P. Pernot[1,2]

[1]Laboratoire de Chimie Physique, CNRS, UMR 8000, Orsay, F-91405

[2]Université Paris-Sud 11, Orsay, F-91405

[3] Laboratoire Interuniversitaire des Systèmes Atmosphériques, CNRS, UMR 7583, Université Paris 7-12, Créteil, F-94010

[4] Space Research Centre, Bartycka 18A, 00-716 Warsaw, POLAND

[5]Laboratoire d'Astrodynamique, d'Astrophysique et d'Aéronomie de Bordeaux, CNRS, UMR 5804, Université Bordeaux 1, Floirac, F-33270

Number of manuscript pages: 30

Number of figures: 8

Number of tables: 1

Running head: Influence of neutral transport on Titan ion chemistry

Corresponding author:

Pascal Pernot

Laboratoire de Chimie Physique

Bat. 349, Université Paris-Sud 11

91405 Orsay Cedex

France

E-mail address: pascal.pernot@lcp.u-psud.fr

Abstract

Models of Titan ionospheric chemistry have shown that ion densities depend strongly on the neutral composition. The turbulent diffusion transport conditions, as modeled by eddy coefficients, can spectacularly affect the uncertainty on predicted neutral densities. In order to evaluate the error budget on ion densities predicted by photochemical models, we perform uncertainty propagation of neutral densities by Monte Carlo sampling and assess their sensitivity to two turbulent diffusion profiles, corresponding to the extreme profiles at high altitudes described in the literature. A strong sensitivity of the ion density uncertainties to transport is observed, generally more important than to ion-molecule reaction parameters themselves. This highlights the necessity to constrain eddy diffusion profiles for Titan ionosphere, which should progressively be done thanks to the present and future measurements of the orbiter Cassini.

Key Words: Atmosphere chemistry, Atmosphere composition, Atmosphere dynamics, Ionospheres, Titan.

1 Introduction

Discrepancies between the outputs of different models and available data are difficult to assess in the absence of quantified uncertainties. In particular, modelling the chemistry of planetary ionospheres involves numerous physical and chemical parameters, which values are known from laboratory measurements with experimental uncertainty factors. These uncertainty sources should be accounted for in the modelling, in order to quantify the uncertainties on the model outputs and more generally to evaluate the model predictivity (Wakelam et al. 2005; Zádor et al. 2006; Hébrard et al. 2007).

In a previous work (Carrasco et al. 2006), we evaluated the uncertainties on a Titan ionospheric chemistry model (based on the work of Banaszkiewicz et al., 2000), due to the rate constants and branching ratios of ion-molecule reactions. Neutral densities were considered as fixed inputs, with the neutral density profiles calculated by Lara et al. (1996). In parallel, Hébrard et al. (2007) studied the chemical kinetics uncertainties in a photochemical model for neutral species in Titan atmosphere. Considering that ion densities closely depend on the neutral atmosphere composition (Keller et al. 1998), one can expect a direct impact of neutral uncertainties on ion uncertainties. In order to evaluate this influence, we built a semi-coupled Titan ionospheric model for neutral and ion species, using the chemistry model described in Carrasco et al. 2006 with neutral density profiles and their uncertainties as calculated by Hébrard et al. (2007).

Dynamics plays undoubtedly some role in the distribution of Titan's both neutral and ionic constituents but yet, the significance of eddy diffusion processes is not entirely known and still requires some attention. The eddy diffusion coefficient $K(z)$ usually acts in photochemical modeling of planetary atmospheres as a free parameter that must be estimated to fit observations (see Fig. 1). In particular, the eventuality that the globally averaged distribution of Titan's constituents may be accurately and simultaneously described with a single eddy diffusion profile is still discussed

(Wilson and Atreya 2004). Hidayat et al. (1997) inferred a low homopause profile (840 km) from their millimeter observations of HCN vertical profile in much of the lower regions of the atmosphere; Strobel et al. (1992) inferred a higher homopause profile (1040 km) from their analysis of Voyager UVS solar occultation and airglow data; Toublanc et al. (1995) developed a very low homopause profile (680 km) from Toon et al. (1992) profile and adapted it to fit Tanguy et al. (1990) HCN distribution and Voyager UVS data for methane CH_4. This diversity of profiles is in part due to the differences in the chemical scheme adopted by the authors. In fact, Hébrard et al. (2007) showed that the eddy diffusion profile may not currently be constrained as tightly as expected. Uncertainties attached to the computed abundances can be indeed so important that modifying the eddy diffusion coefficient $K(z)$ does not change significantly their agreement with the different abundances inferred from the available observations. It appears moreover that the uncertainty factors of computed abundances are very sensitive to the choice of the eddy diffusion profile adopted, especially to the choice of a high- or low-homopause profile.

[Figure 1 about here.]

In order to assess their effect on ion densities, we considered two turbulent diffusion profiles for the neutral species, corresponding to the extreme profiles at high altitudes described in the literature (Strobel et al. 1992; Toublanc et al. 1995). We first evaluated the uncertainties on the ion densities for both neutral turbulent transport cases, with a fixed ion-molecule chemistry. Then, we calculated the contributions of both uncertainty sources (neutral densities and ion-molecule reaction parameters), and identified the main sources of uncertainty for all the major ions predicted by our model of Titan ionosphere.

2 Methods

2.1 Ion and neutral chemistry semi-coupled models for Titan ionosphere

Titan ionospheric chemistry model (Banaszkiewicz et al. 2000; Carrasco et al. 2006) is semi-coupled with a photochemistry model of neutral species (Hébrard et al., 2007). Neutral density profiles are calculated with their uncertainties by the neutral photochemistry model. These profiles, with their uncertainties, are taken as inputs of the ionospheric chemistry model. Furthermore the correlations between neutral densities are taken into account through their covariance matrix. Density profiles are built with a 5 km scale in the 800-1300 km altitude range.

2.2 Uncertainty propagation

Because of non-linearities in the model and large uncertainties on numerous parameters, chances to be outside the validity range of linear uncertainty propagation are important. To avoid this bias, we used a Monte Carlo sampling method, which requires the definition of a probability density function for input parameters. As their are not correlated, we design separately the probability density functions for the kinetic parameters and for the neutral density profiles.

Uncertainties of kinetic parameters of ion-molecule reactions. The distributions are parametrized from the preferred values and the uncertainties reported in the review of Anicich and McEwan 1997. If an uncertainty value is not given for rate constants, the preferred value is considered as being inaccurate, with a relative uncertainty of 60% (highest uncertainty value reported in the review). The global rate k is depicted by a log-uniform distribution (Carrasco et al. 2006).

As uncertainty is not quantified for branching ratios in the reference review, uncertainty intervals have been defined according to the statistical deviations reported

in Carrasco et al. 2006: 10% for branching ratios larger than 0.5, 30% for branching ratios between 0.1 and 0.5 and 100% for the smaller values. For a few reactions, branching ratios are not reported. In such cases the pathways are considered as equiprobable with an uncertainty of 90%. Branching ratios were previously (Carrasco and Pernot 2007) modeled by Dirichlet distributions, which respect the sum rule for these parameters. In this work, we refine our elicitation of the branching ratios with Dirichlet uniform distributions (DIUD), which have the additional property not to favor any value within the given intervals (see the Appendix).

The sample for probability density function of ion-molecule reaction parameters can be produced with the following procedure. In order to preserve the intrinsic correlation due to the sum rule, partial reaction rates for a reaction with n pathways are produced following three steps:

1. a global rate k is sampled from a log-uniform distribution;
2. the branching ratios, b_i, are sampled from the DIUD method (see Appendix),
3. the partial rate constants, k_i, are products of two random numbers $(k_i = kb_i)_1^n$.

Uncertainties on neutral densities. The different chemical sources of uncertainties in photochemical models of Titan's atmosphere and their associated probability density functions were recently reviewed and evaluated at representative temperatures through a comprehensive cross-examination of extensive reaction rates database (Hébrard et al., 2006) and implemented through a Monte-Carlo procedure into a 1D photochemical model of Titan's neutral atmosphere (Hébrard et al., 2007). A sample of $N_{run} = 500$ density profiles for each neutral species is generated at all altitudes up to 1300 km and stored for analysis. The data are in a three dimensional table

$$\{c_{ijk}; i = 1,\ N_{sp};\ j = 1,\ N_{alt};\ k = 1,\ N_{run}\} \tag{1}$$

where N_{sp} is the number of species, N_{alt} is the size of the altitude grid.

These profiles could be used directly in the 0D ionospheric model. However we preferred to build an intermediate probability density function (PDF) because it provides insight into the structure of neutral densities uncertainties. In addition this procedure enables a much larger number of runs to be used for uncertainty propagation and analysis in ionospheric chemistry. Typically, we found that cumulative density functions for ion densities were satisfyingly converged for 10^4 samples, a number presently out of reach of the 1D model.

To design the PDF for neutral densities, we first analyze their correlation structure. We consider two sources of correlation :

- $\rho^{alt}_{ij,il} = \langle c_{ijk}, c_{ilk} \rangle_k$: spatial correlations for a given species, resulting mainly from continuity laws of chemistry-transport processes, where $\langle ... \rangle_k$ denotes the correlation coefficient calculated over the sample;

- $\rho^{sp}_{il,jl} = \langle c_{ilk}, c_{jlk} \rangle_k$: inter-species correlations, resulting from the chemical processes and mass conservation law.

To account for non-linearities, Rank Correlation Coefficients (RCC) have been used. They convert nonlinear but monotonic relationship into a linear relationship by replacing the values of the sampled inputs/outputs by their respective ranks (Hamby 1994; Helton et al. 2006).

The spatial correlation of densities for a species is linked to the deformations caused to the density profile by chemistry fluctuations. If the density variations are similar at all altitudes (all curves in a sample remain parallel), the RCC should be equal to 1. A negative correlation would indicate opposite variations between two altitudes. We calculated the RCC for altitudes between 800 and 1300 km in the case of Strobel et al. 1992 eddy diffusion profile. As expected, spatial correlation is high: for all species, $\rho^{alt}_{ij,il}$ is above 0.4, and for most species, the RCC distribution over altitudes is strongly peaked at the maximal value. Globally, when a species undergoes a density increase/decrease at the base of the ionosphere, there is a similar

increase/decrease in all the upper column. As we are performing 0D calculations for ionospheric chemistry, we can assume that it is safe to consider that all altitudes are maximally correlated, $\rho^{alt}_{ij,il}$=1 for all altitude-pairs and species.

To evaluate the correlation between neutral densities, we chose an altitude representative for ionospheric chemistry, *i.e.* 1200 km, and RCC's for all pairs of species have been evaluated at that altitude. We checked that the RCC's matrix was globally constant in the ionospheric altitude range. It appears that some neutral densities are significantly correlated. A good approximation of the correlation matrix was obtained by using the linear correlations between the log-densities $\log_{10} c_{il}$. This representative correlation matrix was used at every altitudes. The probability density function is thus finally built as a multivariate normal density, parametrized by the average values $\overline{\log_{10} c_{il}}$ and uncertainty factors F_{il}, such as $\log_{10} c_{il} = \overline{\log_{10} c_{il}} \pm \log_{10} F_{il}$, and the correlation matrix with elements $\rho^{sp}_{il,jl}$.

The sample for the full neutral densities probability density function, assuming unity correlation between altitudes and altitude-independent inter-species correlations, can be produced with the following procedure:

- Initializations:
  - estimate average values and uncertainty factors of log-densities for all species, at all altitudes;
  - evaluate inter-species linear correlation matrix of log-densities $\mathbf{C}$ at a representative altitude and calculate its Cholesky decomposition (Gelman et al., 1995).
- Monte Carlo loop:
  - generates N_{sp} standard normal deviates $\{u_i \sim N(0,1);\, i = 1,\, N_{sp}\}$;
  - combines these into N_{sp} correlated numbers ε_i by the Cholesky procedure;
  - loop over altitudes (j);

* generates samples of correlated log-densities with altitude dependent uncertainties $\left\{\log_{10} c_{ij} = \overline{\log_{10} c_{ij}} + \varepsilon_i \times \log_{10} F_{ij};\ i = 1,\ N_{sp}\right\}$.

3 Results and Discussion

3.1 Correlation of neutral densities

[Table 1 about here.]

We evaluated the correlation between the neutral density profiles in the Strobel case. Representative values for some important species are reported in Table 1. Strong correlations are observed between some neutrals, *e.g.* H_2/CH_4, N_2/CH_4 or C_2H_2/C_2H_4, and result from the chemical network. A salient feature is the negative correlation of CH_4 with all other species in the table (increasing the density of CH_4 causes a decrease in the density of those species). The strong negative correlation of CH_4 with N_2 and H_2 has probably not a chemical origin, but a physical one, *i.e.* mass conservation. Full exploration of the other correlation is not relevant to the present study, but will be detailed in a future article. A consequence to be kept in mind for data fitting is that, within the framework of a consistent photochemical model, densities of species should not be adjusted independently of each other. For this study, we conclude that those strong correlations cannot be *a priori* neglected in the uncertainty propagation to ionospheric chemistry.

In order to check this point, we generated two samples in the Strobel case, one correlated and one uncorrelated (setting the correlation matrix to identity: $\mathbf{C} = \mathrm{I}$). We compared the densities and their uncertainties obtained with the two samples. The effect is illustrated on the 40 most abundant ions (Fig. 2). Except for very few ions, the impact is negligible. Predicted ion densities and uncertainties are practically insensitive to the correlation of neutral densities.

[Figure 2 about here.]

A significant effect can however be observed on the correlation between ion densities, as can be seen from the compared cumulative density functions of correlation coefficients of all ions pairs on Fig. 3. For uncorrelated neutral densities, the RCC's are globally weak, massively located, with 90% probability, between -0.1 and 0.6, whereas for the correlated case the corresponding probability interval spreads between -0.3 and 0.8. The proportion of significant correlations increases thus notably when neutrals correlation is taken into account. We observe therefore a correlation transfer from neutrals to ions. This might be relevant for the computation of observables combining ion densities. As observed before, this correlation restricts considerably the degrees of freedom when, for instance, adjusting the ion densities to match an observable (as an ion mass spectrum).

[Figure 3 about here.]

In conclusion to this section, we note that correlation between neutral densities has certainly to be taken into account for data fitting or sensitivity analysis, but that it can safely be neglected for the sole purpose of uncertainty propagation.

3.2 Effect of the neutral transport processes on the ion concentrations

As shown in Hébrard et al. (2007), the turbulent macroscopic transport of the neutral species in Titan ionosphere is not yet tightly constrained by the existing observations and might vary between two extreme cases described in Strobel et al. (1992) and Toublanc et al. (1995). For simplicity, these two cases will be called the "Strobel case" and the "Toublanc case". The eddy coefficient profiles are given on Fig. 1. The Strobel case corresponds to a high homopause level (1040 km) whereas the Toublanc case corresponds to a low homopause level (680 km). The two corresponding neutral density profiles obtained by Hébrard et al. (2007), for diurnally averaged chemistry,

were used as inputs of our simulations, allowing us to evaluate the impact of the poorly known neutral transport processes on the ionic species.

The density profile of the major ion , $HCNH^+$ in Titan ionosphere, is represented on Fig. 4 for both neutral transport cases. The nominal profiles are significantly different for altitudes lower than 950 km: $HCNH^+$ density is up to 10 times larger at 800 km in the Strobel case. This confirms the sensitivity of the ionospheric chemistry model to the neutral density profiles previously noticed by Keller et al. (1998). Moreover, the uncertainties on $HCNH^+$ density differ significantly from one case to the other, with a larger uncertainty in the Toublanc case, at all altitudes.

[Figure 4 about here.]

The altitude 1200 km is of specific interest, being the average altitude of the first Cassini's flyby T5 providing data on ion densities. We compared the effect of both neutral diffusion cases on the ten major ions calculated by our model at this altitude: $HCNH^+$, $C_2H_5^+$, CH_5^+, N_2^+, $C_3H_5^+$, CH_3^+, N_2H^+, $N(^3P)^+$, $C_2H_4^+$ and $C_2H_3^+$. The densities with their uncertainties are reported on Fig. 5. The ions are ranked by decreasing density. The results are highly dependent on the eddy diffusion profile: quite precise ion densities in the Strobel case, and relative uncertainties of one or two orders of magnitude for all ions in the Toublanc case.

[Figure 5 about here.]

One can conclude that the eddy coefficient chosen to describe the transport of the neutral species influences significantly the nominal density profiles of the ion species but also their uncertainty. The chemistry of the ions in Titan ionosphere cannot be decorrelated from transport considerations.

There is still to understand why the uncertainties in the Toublanc case are much larger than in the Strobel case. A reason lies probably in the uncertainty on the major neutral reactant, methane (CH_4). Indeed the uncertainty on the methane

profiles at the ionospheric altitudes is substantially larger in the Toublanc case (see Fig. 6). The uncertainty factor F_{CH_4} at 1200 km is equal to about 1.1 in the Strobel case and about 5.7 in the Toublanc case. High-homopause profiles seem to restrain to some extent the propagation of chemical uncertainties in the upper atmosphere contrary to low-homopause profiles.

[Figure 6 about here.]

The reason for such a discrepancy on methane uncertainty is not yet fully established. However, the vertical transport is more important in the case of a high homopause. This means that the vertical renewal of the species through transport, compensates more efficiently for the chemical losses. The transport can thus be considered as an attenuation factor of the chemical uncertainties on the neutral densities.

3.3 Comparison of two uncertainty sources: neutral densities and ion-molecule reactions parameters

We compared the respective contributions of the neutral densities and of the parameters of ion-molecule reactions to the ion density uncertainty by first performing uncertainty propagation on both uncertainty sources separately. As earlier, both Strobel and Toublanc cases were considered to encompass extreme transport processes in Titan ionosphere.

The ten major ion densities are reported in Fig. 7, with their uncertainties for both Strobel and Toublanc cases. Each case is compared with the uncertainty contribution of the ion-molecule reaction parameters. In the Toublanc case, the uncertainty due to the ion-molecule reaction parameters is negligible in comparison to the uncertainty due to the neutral densities. This implies that in this case, the uncertainty on the ion densities is mainly controlled by the uncertainty on the neutral atmosphere rather than by the ion reactivity itself. In the Strobel case,

similar amplitudes for both uncertainty sources are observed. The conclusions are therefore depending on the ions: a prevalence of the neutral density uncertainty is observed for $C_3H_5^+$ and $C_2H_3^+$, whereas a prevalence of the ion-molecule reaction parameters is observed for $C_2H_4^+$. Similar contribution of both uncertainty sources affect $HCNH^+$, $C_2H_5^+$, CH_5^+, N_2^+, CH_3^+, N_2H^+, and $N(^3P)^+$.

[Figure 7 about here.]

The Strobel case corresponds to a high homopause configuration. One can notice that the hypothesis of a high homopause seems to be consolidated by the recent INMS data (Yelle et al., 2006).

4 Conclusion

We presented the first evidence of the influence of the modeling of turbulent transport of neutral species on the uncertainty of ion chemistry in Titan ionosphere.

We found a strong sensitivity of ion chemistry to the description of turbulent neutral transport. The uncertainties on the ion densities were much higher with a low homopause hypothesis than with a high homopause level. This effect can be explained by a competition between vertical transport and chemistry: an efficient vertical transport attenuates the chemical uncertainties. In the case of a low homopause, the uncertainty of the ion densities due to the ion chemistry was even found negligible in comparison to the uncertainty due to the neutral densities. This highlights the necessity to constrain eddy diffusion profiles for Titan ionosphere, which should progressively be done thanks to the present and future measurements of the Cassini orbiter (Yelle et al. 2006).

The present study focused on the sensitivity of a Titan ionospheric model to two particular sources of uncertainty: the description of the neutral density profiles, and the ion-molecule chemistry parameters. Additional sources of uncertainty are still to be studied, such as uncertainties on the photo-dissociation or recombination

rates, which would allow a complete overview of the needs and limits of the actual model, in order to improve it.

We showed that neutral species are strongly correlated by the photochemical model and transfer an important correlation between ion densities. This provides chemistry-based constraints that might be useful when trying to fit models to measured Mass Spectra, for instance by tuning neutral densities.

The present simulations provide a basis for a sensitivity analysis, from which to identify the key reactions and species strongly responsible for outputs uncertainty. In a forthcoming paper, we will present results along this line, pertaining to both ion-molecule and neutral chemistry.

Appendix:

Dirichlet Uniform Distribution (DIUD) for branching ratios of ion-molecule reactions

An elicitation scheme is based on considerations about the nature of the uncertainties to be represented. Branching ratios are often specified by intervals (Jenkinson 2005; Bates et al. 2003), and it is assumed that there is no reason to favor any value within a given interval. This case seems indeed to be the one favored by experts in the measurement of branching ratios. They consider that they report intervals accounting for systematic errors with enough latitude to encompass all acceptable values (Carrasco et al. 2006).

The distribution is defined uniformly over the $(n-1)$-simplex

$$(b_1, \ldots, b_n) \sim \text{Dirichlet}(1, \ldots, 1) \tag{2}$$

with an additional set of constraints,

$$b_i \in [b_{i,min}, b_{i,max}] \tag{3}$$

The definition of the limits of the intervals depends on the available information. If one gets a set as $(\overline{b}_i, \triangle\overline{b}_i)_{i=1}^n$, one has simply $b_{i,min} = \overline{b}_i - \Delta\overline{b}_i$ and $b_{i,max} = \overline{b}_i + \Delta\overline{b}_i$. For the sake of convenience, we name this truncated uniform Dirichlet distribution DIUD in the following. It has $2n$ parameters

$$(b_1, \ldots, b_n) \sim \mathrm{DIUD}(\overline{b}_1, \ldots, \overline{b}_n, \Delta\overline{b}_1, \ldots, \Delta\overline{b}_n) \tag{4}$$

Samples corresponding to the same branching ratios $(0.6, 0.3, 0.1)$ for 10% and 90% relative uncertainty are displayed in Fig. 8. Note that, although the distribution is uniform over the restricted $(n-1)$-simplex, this is not the case for the marginal distributions.

The most thorough method to produce samples from this distribution is to draw samples from the uniform Dirichlet distribution (generated by the Gamma algorithm, Gelman et al. 1995) and to reject those lying outside the prescribed intervals. However for fairly accurate branching ratios, this method can spill a lot of random draws.

[Figure 8 about here.]

Acknowledgments

This work was partly supported by EuroPlaNet through travel grants to M.D. and M.B. We also acknowledge the support received from Centre National de Recherche Scientifique (CNRS) and from Centre National d'Etude Spatiale (CNES) through postdoctoral positions for N.C. We gratefully thank O. Dutuit, R. Thissen and C. Alcaraz for fruitful discussions.

References

Anicich, V., McEwan, M., 1997. Ion-molecule chemistry in Titan's ionosphere. Planetary and Space Science 45 (8), 897–921.

Banaszkiewicz, M., Lara, L., Rodrigo, R., Lopez-Moreno, J., Molina-Cuberos, G., 2000. A coupled model of Titan's atmosphere and ionosphere. Icarus 147, 386–404.

Bates, S., Cullen, A., Raftery, A., 2003. Bayesian uncertainty assessment in multicompartment deterministic simulation models for environmental risk assessment. Environmetrics 14, 355–371.

Carrasco, N., Dutuit, O., Thissen, R., Banaszkiewicz, M., Pernot, P., 2006. Uncertainty analysis of bimolecular reactions in Titan ionosphere chemistry model. Planetary and Space Science 55, 141–157.

Carrasco, N., Pernot, P., 2007. Modeling of branching ratio uncertainty in chemical networks by dirichlet distributions. Journal of Physical Chemistry A in press.

Gelman, A., Carlin, J. B., Stern, H. S., Rubin, D. B., 1995. *Bayesian Data Analysis*. Chapman & Hall, London.

Hamby, D., 1994. A review of techniques for parameter sensitivity analysis of environmental models. Environmental Monitoring and Assessment 32, 135–154.

Hébrard, E., Dobrijevic, M., Bénilan, Y., Raulin, F., 2006. Photochemical kinetics uncertainties in modeling Titan's atmosphere: a review. Journal of Photochemistry and Photobiology C: Photochemistry Reviews 7, 211–230.

Hébrard, E., Dobrijevic, M., Bénilan, Y., Raulin, F., 2007. Consequences of chemical kinetics uncertainties in modeling Titan's atmosphere. Planetary and Space Science accepted.

Helton, J., Johnson, J., Sallaberry, C., Storlie, C., 2006. Survey of sampling-based methods for uncertainty and sensitivity analysis. Reliability Engineering and System Safety 91, 1175–1209.

Hidayat, T., Marten, A., Bézard, B., Gautier, D., Owen, T., Matthews, H., Paubert, G., 1997. Millimeter and submillimeter heterodyne observations of Titan: Retrieval of the vertical profile of HCN and the 12C/13C solar ratio. Icarus 126 (1), 170–182.

Jenkinson, D., 2005. The elicitation of probabilities - A review of the statistical literature. BEEP working paper, University of Sheffield.

Keller, N. G., Anicich, V. G., Cravens, T. E., 1998. Model of Titan's ionosphere with detailed hydrocarbon ion chemistry. Planetary and Space Science 46, 1157.

Lara, L., Lellouch, E., Lopez-Moreno, J., Rodrigo, R., 1996. Vertical distribution of titan's atmospheric neutral constituents. J. Geophys. Res. 101 (23261-23283).

Strobel, D. F., Summers, M., Zhu, X., 1992. Titan's upper atmosphere: structure and ultraviolet emissions. Icarus 100, 512–526.

Tanguy, L., Bézard, B., Marten, A., Gautier, D., Gérard, E., Paubert, G., Lecacheux, A., 1990. Stratospheric profile of HCN on Titan from millimeter observations. Icarus 85, 43–57.

Toon, O., McKay, C., Griffith, C., Turco, R., 1992. A physical model of Titan's aerosols. Icarus 95, 24–53.

Toublanc, D., Parisot, J., Brillet, J., Gautier, D., Raulin, F., McKay, C., 1995. Photochemical modeling of Titan's atmosphere. Icarus 113, 2–26.

Wakelam, V., Selsis, F., Herbst, E., Caselli, P., 2005. Estimation and reduction of the uncertainties in chemical models: application to hot core chemistry. A. & A. 444, 883–891.

Wilson, E., Atreya, S., 2004. Current state of modeling the photochemistry of Titan's mutually dependent atmosphere and ionosphere. Journal of Geophysical Research 109.

Yelle, R., Borggren, N., de La Haye, V., Kasprzak, W., Niemann, H., Müller-Wodarg, I., Waite, J., 2006. The vertical structure of Titan's upper atmosphere from Cassini Ion Neutral Mass Spectrometer measurements. Icarus 182 (2), 567–576.

Zádor, J., Zsély, I., Turányi, T., 2006. Local and global uncertainty analysis of complex chemical kinetic systems. Reliability Engineering and System Safety 91, 1232–1240.

	CH4	C2H2	C2H4	C2H6	N2	HCN
H2	**-0.85**	0.23	0.41	0.31	**0.86**	**0.52**
CH4		-0.20	-0.45	**-0.56**	**-0.99**	**-0.69**
C2H2			**0.84**	0.15	0.13	0.02
C2H4				0.25	0.40	0.19
C2H6					**0.56**	0.43
N2						**0.68**

Table 1: Rank correlation coefficients between selected neutral densities at 1200 km. Coefficients with an absolute value above 0.5 are in bold face.

List of Figures

1 Eddy diffusion profiles - Hidayat et al. (1997) profile (solid line), Strobel et al. (1992) profile (dashed line) and Toublanc et al. (1995) profile (dot dashed line). The methane molecular diffusion coefficient profile is also included. 22

2 Effect of inter-species correlation of neutral species on ion densities at 1200 km with a Strobel et al. (1992) eddy diffusion profile: the ion densities of the 40 most abundant ions are depicted. Empty boxes: no correlation, Filled boxes: correlation. 23

3 Inter-species rank correlation coefficients for the densities of ions of the ionospheric model at 1200 km: empirical cumulative density function (CDF) for all pairs of ions. Dashed line: uncorrelated neutral densities; plain line : correlated case. 24

4 Density profiles of $HCNH^+$: (a) with Strobel et al. eddy coefficient ; (b) with Toublanc et al. eddy coefficient. 25

5 Densities of the ten major ions at altitude 1200 km for the two eddy coefficients. Boxplots depict 50% and 90% confidence intervals. For each ion density, the upper boxplot corresponds to the Toublanc case, whereas the lower boxplot depicts uncertainty propagation in the Strobel case. 26

6 Density profile of methane in Titan ionosphere (a) in the Strobel case, (b) in the Toublanc case. 27

7 Densities of the ten major ions at altitude 1200 km for the two eddy coefficients : (a) Strobel case, (b) Toublanc case. Boxplots depict 50% and 90% confidence intervals. For each ion density, the upper boxplot corresponds to uncertainty propagation of the neutral density, whereas the lower boxplot depicts uncertainty propagation of ion chemistry parameters. 28

8 Samples and marginals from Dirichlet distributions: (a) 10% relative uncertainty $(b_1, b_2, b_3) \sim \mathrm{DIUD}\left((0.6, 0.3, 0.1), (0.06, 0.03, 0.01)\right)$; (b) 90% relative uncertainty $(b_1, b_2, b_3) \sim \mathrm{DIUD}\left((0.6, 0.3, 0.1), (0.54, 0.27, 0.09)\right)$. 29

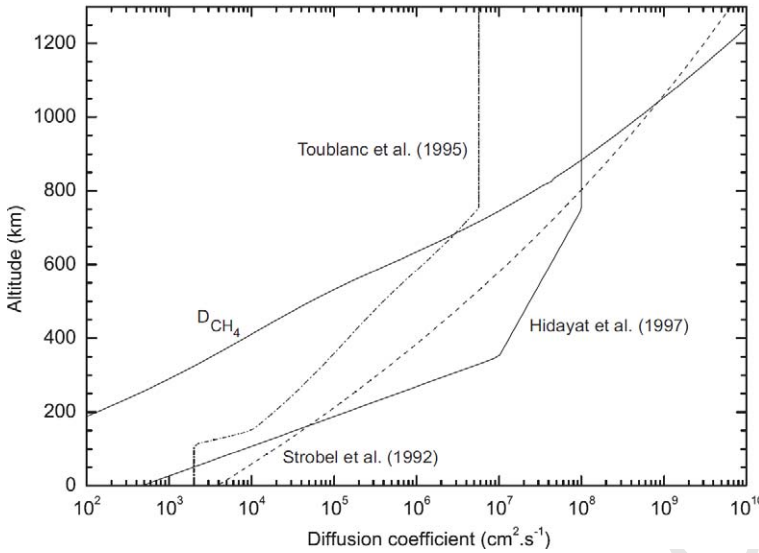

Figure 1: Eddy diffusion profiles - Hidayat et al. (1997) profile (solid line), Strobel et al. (1992) profile (dashed line) and Toublanc et al. (1995) profile (dot dashed line). The methane molecular diffusion coefficient profile is also included.

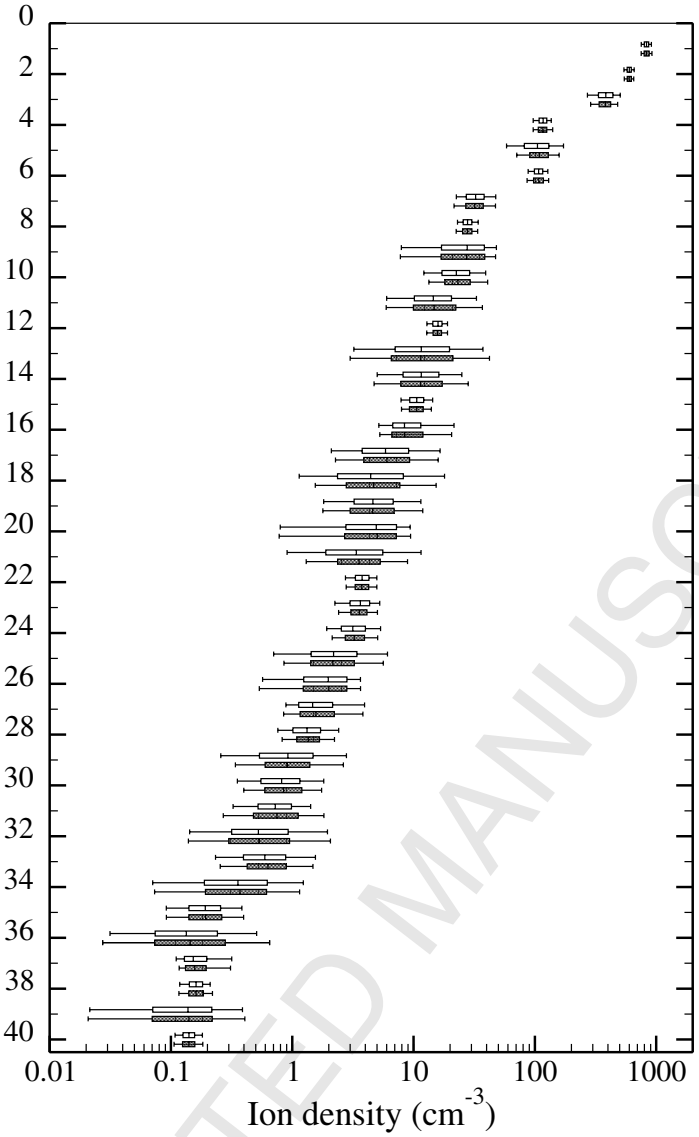

FIG. 2 – Effect of inter-species correlation of neutral species on ion densities at 1200 km with a Strobel et al. (1992) eddy diffusion profile: the ion densities of the 40 most abundant ions are depicted. Empty boxes: no correlation, Filled boxes: correlation.

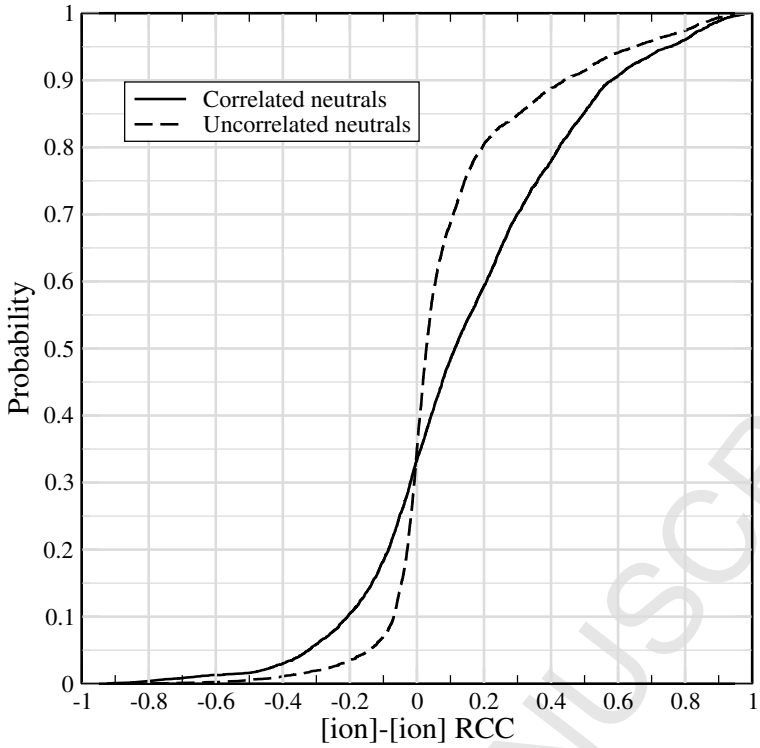

Figure 3: Inter-species rank correlation coefficients for the densities of ions of the ionospheric model at 1200 km: empirical cumulative density function (CDF) for all pairs of ions. Dashed line: uncorrelated neutral densities; plain line : correlated case.

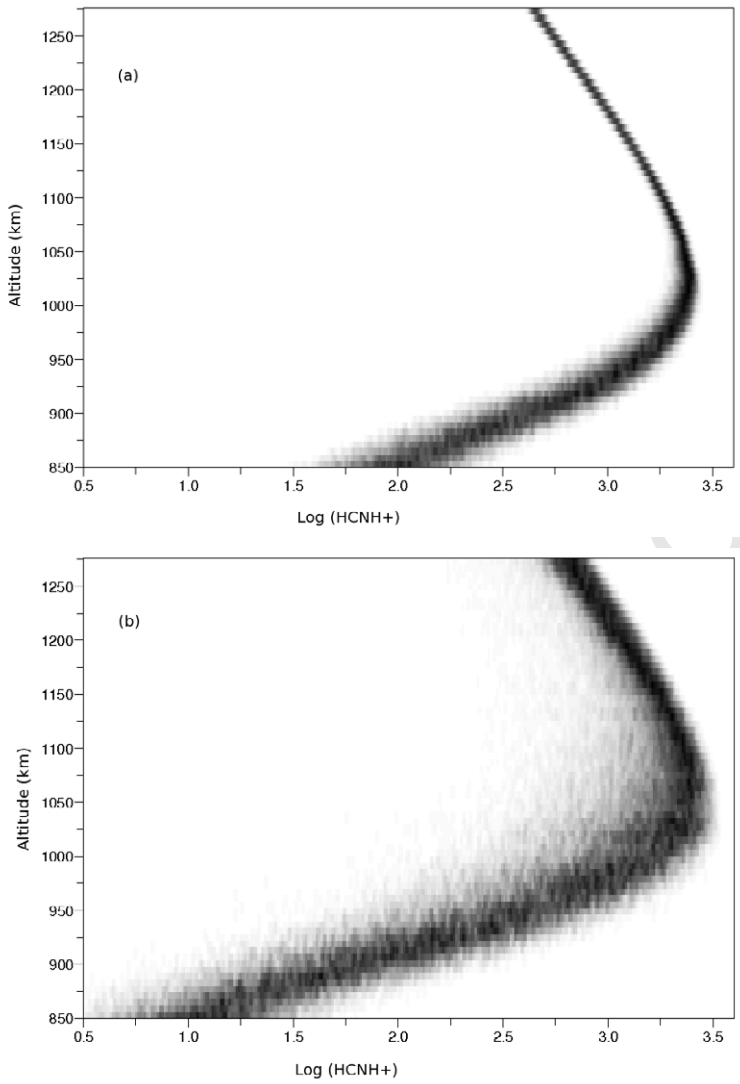

Figure 4: Density profiles of $HCNH^+$: (a) with Strobel et al. eddy coefficient ; (b) with Toublanc et al. eddy coefficient.

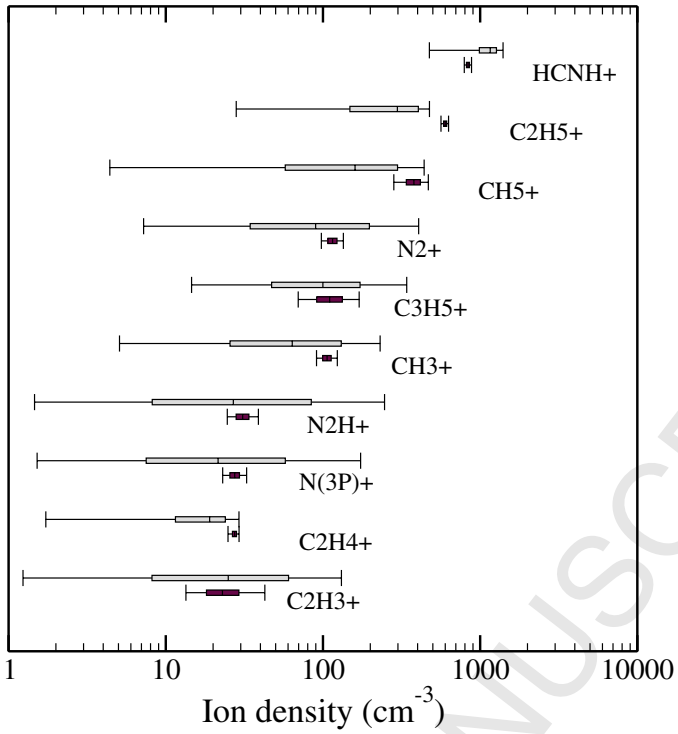

Figure 5: Densities of the ten major ions at altitude 1200 km for the two eddy coefficients. Boxplots depict 50% and 90% confidence intervals. For each ion density, the upper boxplot corresponds to the Toublanc case, whereas the lower boxplot depicts uncertainty propagation in the Strobel case.

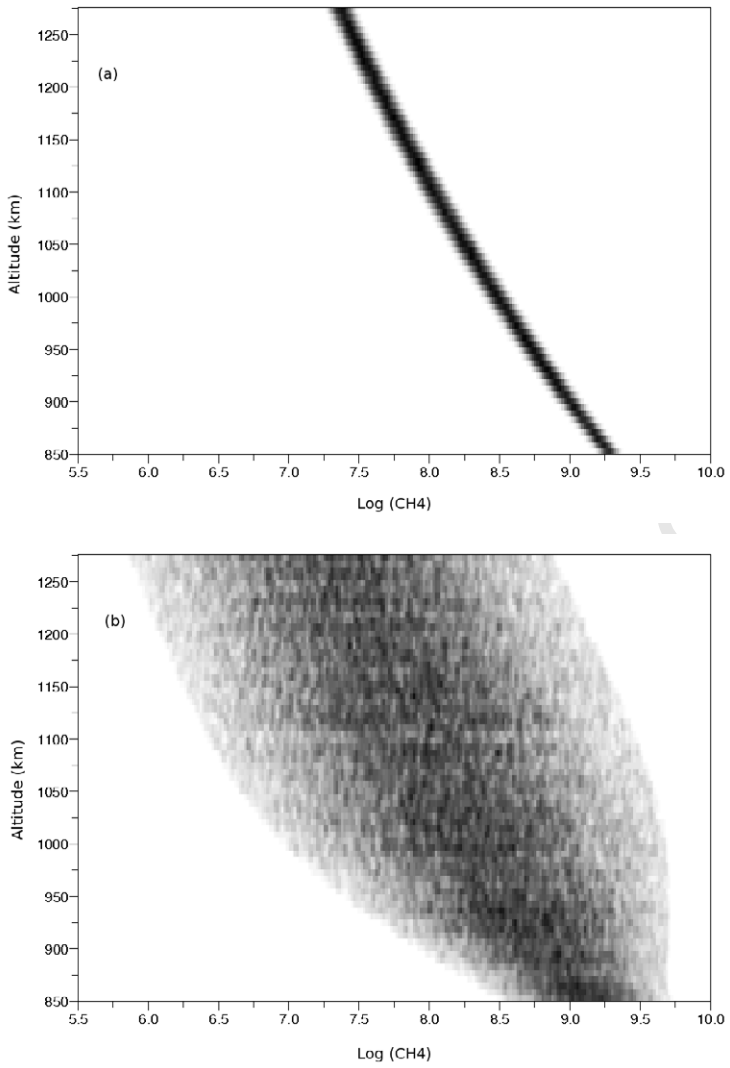

Figure 6: Density profile of methane in Titan ionosphere (a) in the Strobel case, (b) in the Toublanc case.

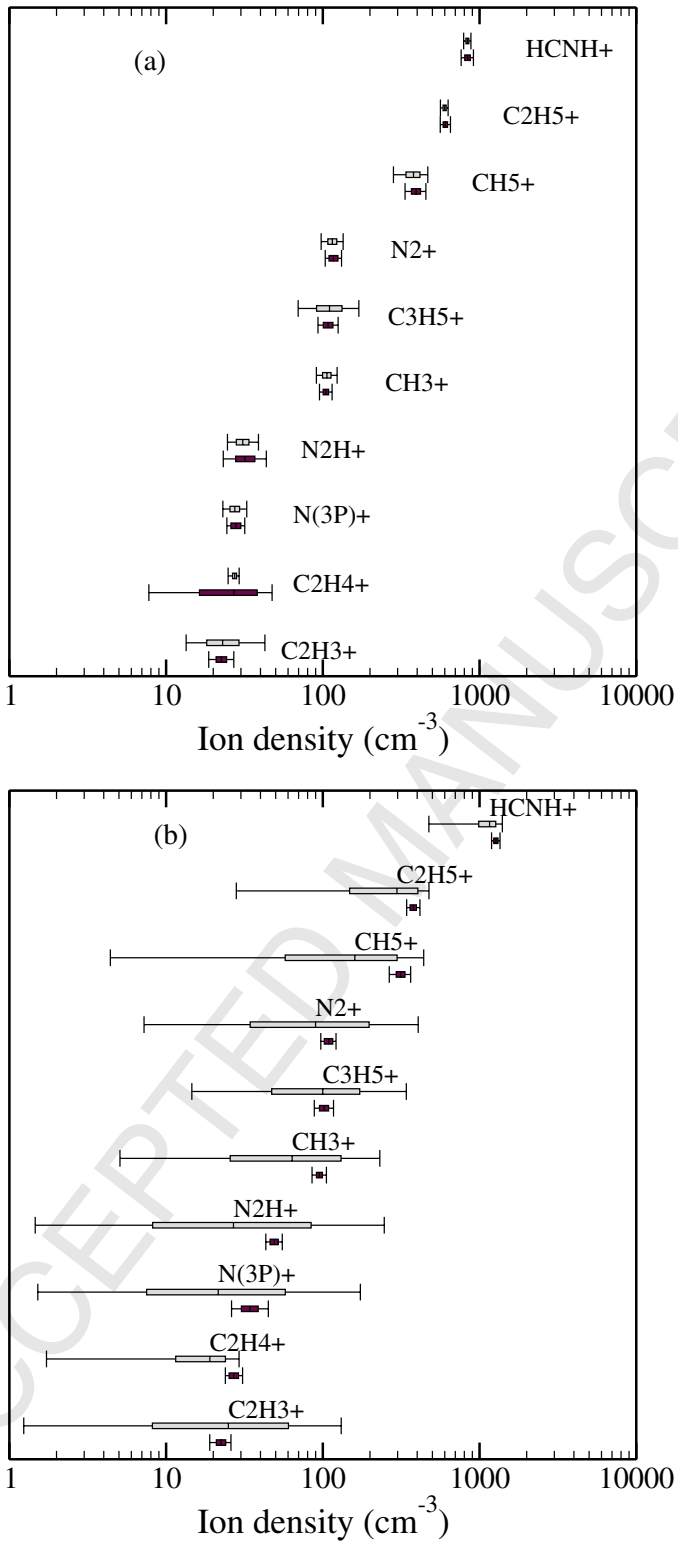

Figure 7: Densities of the ten major ions at altitude 1200 km for the two eddy coefficients : (a) Strobel case, (b) Toublanc case. Boxplots depict 50% and 90% confidence intervals. For each ion density, the upper boxplot corresponds to uncertainty propagation of the neutral density, whereas the lower boxplot depicts uncertainty propagation of ion chemistry parameters.

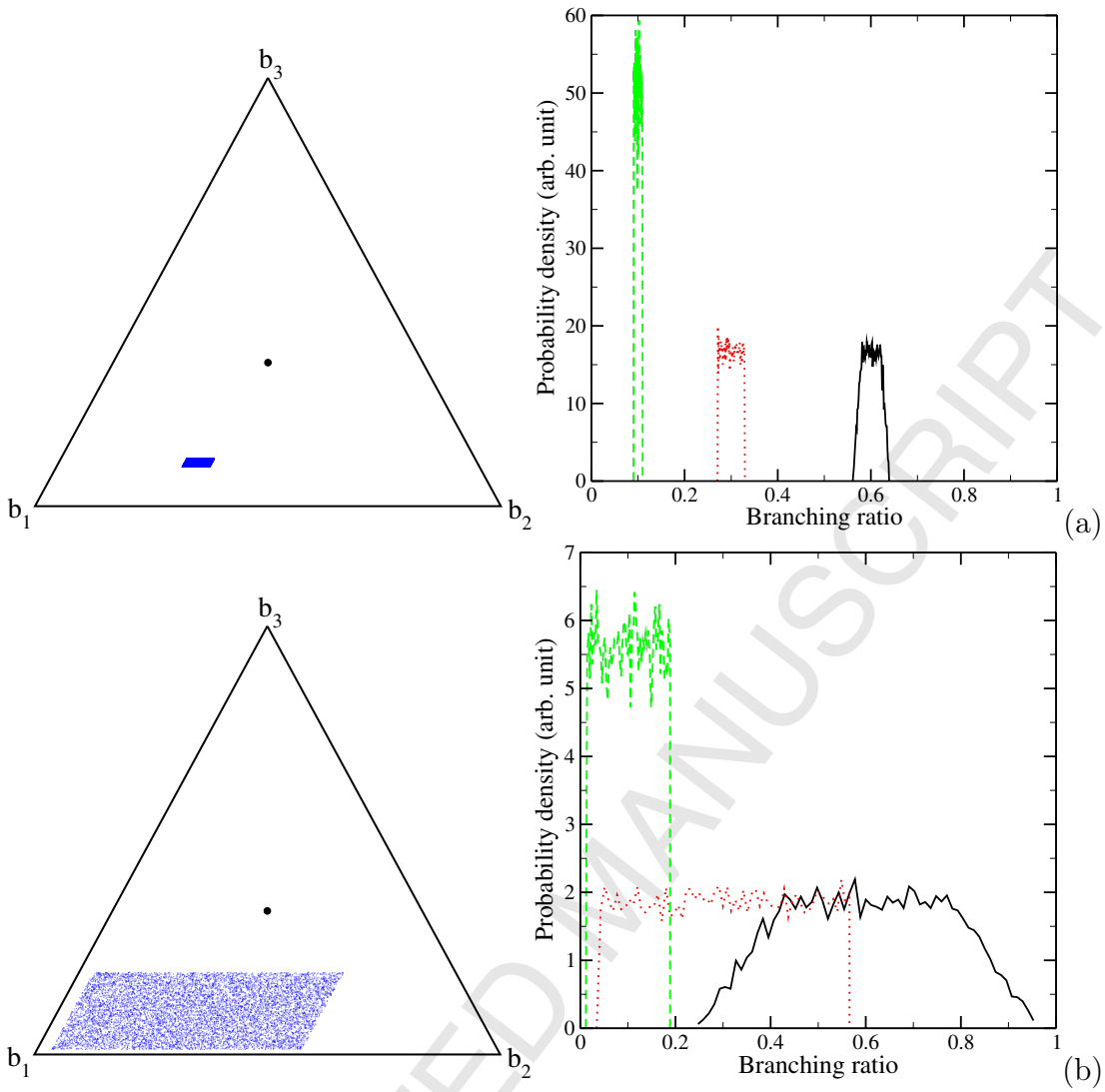

Figure 8: Samples and marginals from Dirichlet distributions: (a) 10% relative uncertainty $(b_1, b_2, b_3) \sim \text{DIUD}\left((0.6, 0.3, 0.1), (0.06, 0.03, 0.01)\right)$; (b) 90% relative uncertainty $(b_1, b_2, b_3) \sim \text{DIUD}\left((0.6, 0.3, 0.1), (0.54, 0.27, 0.09)\right)$.